

## Platinum Stilbazoles: Ring-Walking Coupled with Aryl–Halide Bond Activation

David Strawser,<sup>†</sup> Amir Karton,<sup>†</sup> Olena V. Zenkina,<sup>†</sup> Mark A. Iron,<sup>†</sup> Linda J. W. Shimon,<sup>‡</sup> Jan M. L. Martin,<sup>\*,†</sup> and Milko E. van der Boom<sup>\*,†</sup>

Departments of Organic Chemistry and Chemical Research Support, Weizmann Institute of Science, Rehovot 76100, Israel

Received January 30, 2005; E-mail: comartin@wicc.weizmann.ac.il; milko.vanderboom@weizmann.ac.il

A metal complex “walking” over electron-rich  $\pi$ -conjugated systems is believed to be a key process<sup>1–7</sup> in many chemical transformations involving arene functionalization and activation of strong C–C, C–H, and C–X (X = halide) bonds.<sup>8–11</sup> Despite several experimental<sup>12</sup> and computational studies,<sup>5,13–17</sup> ring-walking is often difficult to prove unambiguously, as the vast majority of metal-promoted arene functionalization reactions are bimolecular, require elevated temperatures, and intermediates are not observed. A detailed mechanistic understanding of metal–arene interactions would lead to the design of new selective metal-mediated processes. We demonstrate here, both by experiment and by Density Functional Theory (DFT) calculations, a selective chemical transformation in which metal coordination to a stilbazole double bond is followed by a ring-walking process prior to intramolecular aryl–halide oxidative addition to a low-valent metal center.

The reaction of 4-[*trans*-2-(4-bromophenyl)vinyl]pyridine (**1**) with a stoichiometric amount of Pt(PEt<sub>3</sub>)<sub>4</sub><sup>18</sup> in dry THF at room temperature for 2 days results in the selective formation of the new complex **2** by  $\eta^2$ -coordination of the metal center to the C=C double bond (Scheme 1). Complex **2** was formed quantitatively as judged by <sup>31</sup>P{<sup>1</sup>H} NMR spectroscopy, isolated as a light yellow solid in 80% yield, and fully characterized by <sup>1</sup>H, <sup>31</sup>P{<sup>1</sup>H}, and <sup>13</sup>C{<sup>1</sup>H} NMR spectroscopy, elemental analysis, mass spectrometry, and single-crystal X-ray crystallography (Figure 1, left).

Yellow crystals of complex **2** were obtained upon slow evaporation of a pentane solution under a nitrogen atmosphere at room temperature. The X-ray structure of **2** in Figure 1 clearly shows the  $\eta^2$ -coordination mode of the metal center to the double bond with the aryl–bromide bond intact.

The reaction of **1** and Pt(PEt<sub>3</sub>)<sub>4</sub> in toluene or THF at 65 °C for 24 h in a sealed pressure vessel results in the quantitative formation of complex **3** by the activation of the aryl–bromide bond (Scheme 1). Complex **3** (Figure 1) was isolated as a white solid (80%) and characterized by the same means as for **2**. For instance, the <sup>31</sup>P{<sup>1</sup>H} NMR spectrum of **3** exhibits one sharp singlet at  $\delta$  11.1 ppm for both <sup>31</sup>P nuclei, flanked by <sup>195</sup>Pt satellites, indicating that both phosphorus atoms are magnetically equivalent. The observed <sup>1</sup>J<sub>PtP</sub> = 2752 Hz is typical of two mutually *trans* phosphorus atoms bound to a d<sup>8</sup> Pt(II) center. The thermolysis of **2** in solution or as a solid at 65 °C also results in the quantitative formation of complex **3**. Thus, metal–olefin coordination is kinetically preferred over the thermodynamically favored aryl–halide bond activation. It is likely that unsaturated platinum complexes are initially formed, which in principle can undergo coordination to the C=C double bond or C–Br oxidative addition.

To probe the mechanism of the formation of complex **3**, a series of in situ <sup>31</sup>P{<sup>1</sup>H} NMR follow-up experiments were done (Figure 2). The reaction **2** → **3**, for which intermediates were not observed,

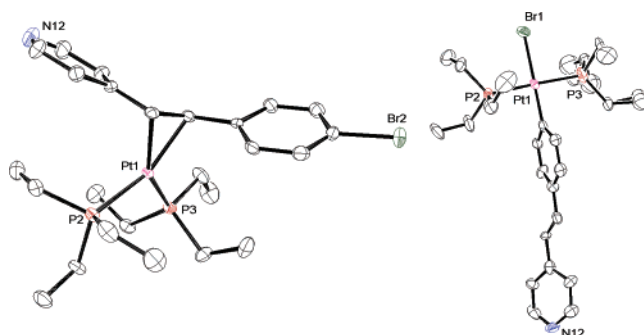


**Figure 1.** ORTEP diagrams of complexes **2** (left) and **3** (right) (thermal ellipsoids set at 50% probability). Bond lengths and angles are given in the Supporting Information.

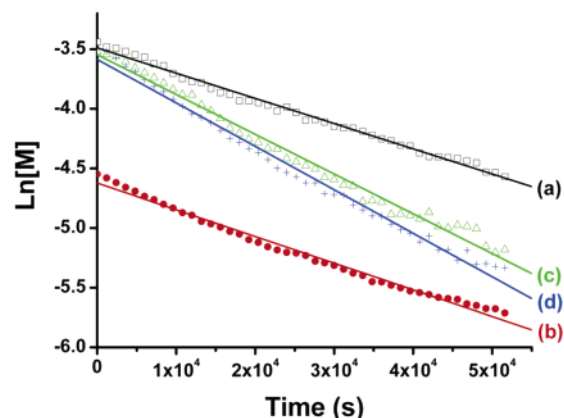
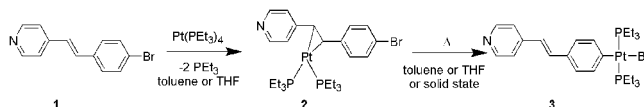


**Figure 2.** Representative in situ <sup>31</sup>P{<sup>1</sup>H} NMR follow-up measurements of the thermolysis of **2** at 331 K: (a) C<sub>6</sub>D<sub>6</sub>, 25 mg/mL,  $k = -2.1 \times 10^{-5} \text{ s}^{-1}$ ,  $R^2 = 0.992$ ; (b) C<sub>6</sub>D<sub>6</sub>, 8.3 mg/mL,  $k = -2.2 \times 10^{-5} \text{ s}^{-1}$ ,  $R^2 = 0.998$ ; (c) THF, 25 mg/mL,  $k = -3.4 \times 10^{-5} \text{ s}^{-1}$ ,  $R^2 = 0.986$ ; (d) THF, 25 mg/mL, 2 equiv of PEt<sub>3</sub>,  $k = -3.6 \times 10^{-5} \text{ s}^{-1}$ ,  $R^2 = 0.997$ .

### Scheme 1



follows first-order kinetics in complex **2**, indicating a unimolecular process. Furthermore,  $t_{1/2}$  ( $3.0 \times 10^{-4} \text{ s}$ ) for the thermolysis of **2** in toluene is independent of the concentration of **2** (0.012–0.072 M) or the presence of excess PEt<sub>3</sub> (2–10 equiv). Therefore, any mechanism involving metal–olefin dissociation and/or a bimolecular reaction can be excluded, as the reaction rates of these pathways should be affected by the concentration and are expected to follow higher-order kinetics. A pathway involving the intermediacy of unsaturated platinum species would have been slowed by the presence of excess PEt<sub>3</sub>. Furthermore, dissociation could lead to the formation of bimetallic species, which were not detected. Moreover, the fluoro

<sup>†</sup> Department of Organic Chemistry.

<sup>‡</sup> Department of Chemical Research Support.

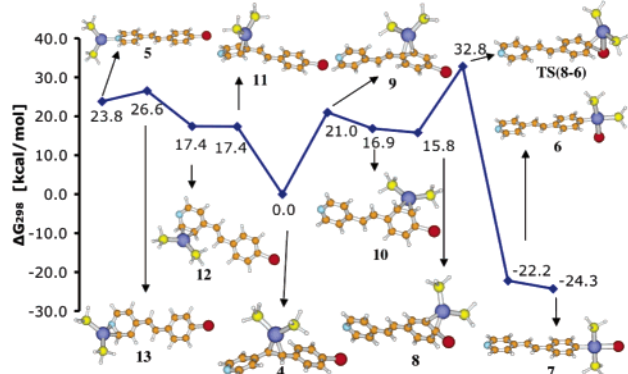


**Figure 3.** Reaction profile (kcal/mol, PCM(THF)-BMK/SDB-cc-pVTZ//BMK/SDD) for the ring-walking and the structures of the various complexes. (Atomic color scheme: C – orange, H – white, Pt – dark blue, N – light blue, Br – red, P – yellow.)

analogue of **2** is stable for at least 2 weeks at 195 °C in THF. Under these conditions, dissociation of  $\text{Pt}(\text{PEt}_3)_2$  is expected to result in nonselective reactions with itself, the solvent, and the ligand. Increasing the solvent polarity (e.g., benzene vs THF) resulted in a rate increase  $k_{\text{THF}}/k_{\text{benzene}} \approx 1.6$  at 331 K. This solvent effect indicates that the rate-determining step in the reaction  $2 \rightarrow 3$  is most probably the oxidative addition of the aryl bromide to the low-valent metal center. It is known that aryl–halide oxidative addition proceeds via a polar transition state whose barrier will be lowered by increasing the solvent polarity.<sup>4</sup> To verify the nature of the rate-determining step, the iodo analogue of **2** was prepared. Its complete conversion to the product of aryl–iodide oxidative addition was observed at room temperature in THF within 2 days, whereas complex **2** is stable under these reaction conditions. This demonstrates that there is a lower activation barrier for the ring-walking process than for oxidative addition. The activation parameters for the thermolysis of **2** (58–78 °C) in toluene were determined from an Eyring plot:  $\Delta H^\ddagger = 16.0 \pm 3$  kcal/mol,  $\Delta S^\ddagger = 130 \pm 4$  eu, and  $\Delta G^\ddagger_{298\text{K}} = 28.2 \pm 4$  kcal/mol.

DFT calculations were performed to support the above mentioned findings.<sup>19,20</sup> For reasons of computational cost,  $\text{PEt}_3$  was substituted by  $\text{PH}_3$ . Ten local minima were located on the potential energy surface (PES, Figure 3), seven of which correspond to  $\eta^2$ -coordination of  $\text{Pt}(\text{PH}_3)_2$  to the bridging double bond (**4**), the phenyl, and the pyridine. The remaining local minima correspond to  $\eta^1$ -coordination of  $\text{Pt}(\text{PH}_3)_2$  to the pyridine nitrogen (**5**) and the cis (**6**) and trans (**7**) oxidative addition products. The transition state, **TS(8–6)**, between the  $\text{Pt}(\text{PH}_3)_2$   $\eta^2$ -coordinated to  $\text{C}_{\text{Br}}-\text{C}_{\text{ortho}}$  bond of the benzene ring (**8**) and **6** was located as was **TS(4-diss)** for the dissociation of  $\text{Pt}(\text{PH}_3)_2$  from **4**.

The PES is characterized by an energy well around **4** (Figure 3), which was chosen as the zero-energy reference point. The  $\eta^2$ -coordination of the metal center to either aromatic ring is higher by  $\Delta G_{298\text{K}} = 16\text{--}26$  kcal/mol. The transition state for oxidative addition has a relative energy of  $\Delta G^\ddagger_{298\text{K}} = 32.8$  kcal/mol. The cis (**6**) and trans (**7**) oxidative addition products are lower in energy by  $\Delta G_{298\text{K}} = -22.2$  and  $-24.3$  kcal/mol, respectively.

Coordination of  $\text{Pt}(\text{PH}_3)_2$  to either ring disrupts the aromaticity,<sup>21</sup> as indicated by the changes in bond lengths in comparison to those of the free ligand (**1**) (see Supporting Information). Coordination of the metal center to a C–C bond of the phenyl ring results in lengthening of the adjacent and opposite C–C bonds by  $\sim 0.05$  Å and shortening of the other two by  $\sim 0.03$  Å. In addition, the hydrogens bonded to the  $\eta^2$ -coordinated carbons are bent out of the plane of the ring by  $\sim 24^\circ$ . This may account (at least partially) for the relative stability of **4**.

Dissociation<sup>22,23</sup> of  $\text{Pt}(\text{PH}_3)_2$  from **4** was calculated to have a  $\Delta G_{298\text{K}} = 3.9$  kcal/mol. A transition state for this reaction was found to lead to a reaction barrier of  $\Delta G^\ddagger_{298\text{K}} = 22.2$  kcal/mol, while migration from **4** to **9** ( $\eta^2$ -coordinated to the  $\text{C}_{\text{para}}-\text{C}_{\text{meta}}$  bond of the benzene ring) is  $\Delta G^\ddagger_{298\text{K}} = 21.0$  kcal/mol. Dissociation from **8** has a barrier of  $\Delta G^\ddagger_{298\text{K}} = 9.7$  kcal/mol, which is lower than that of **TS(8–6)** ( $\Delta G^\ddagger_{298\text{K}} = 17.0$  kcal/mol). The energy of this “loose” transition state should be taken with caution because of (a) the fundamental deficiencies of DFT for dispersion interactions, and (b) inordinate sensitivity to the geometry. Stable  $\eta^2$ -arene complexes are known.<sup>1–7</sup> Phosphine dissociation from arene complex **10** has a high reaction barrier ( $\Delta G^\ddagger_{298\text{K}} = 31.4$  kcal/mol).

In summary, olefin coordination to a zero-valent platinum complex is kinetically favored over aryl–halide oxidative addition. The transformation of  $2 \rightarrow 3$  proceeds both in solution and in the solid state. Contrary to what one would expect based on textbook organometallic transformations, the experimental data demonstrate that a metal–olefin dissociation mechanism followed by aryl–halide bond activation does not occur. Instead, the metal center walks over the  $\pi$ -conjugated ring system until it reaches and activates the aryl–halide bond. DFT calculations support such a premise, although  $\text{Pt}(\text{PH}_3)_2$  dissociation could not be conclusively ruled out. The implications of these findings for other late transition metal complexes and other  $\pi$ -conjugated ligand systems are currently under investigation.

**Acknowledgment.** Research was supported by the Helen and Martin Kimmel Center for Molecular Design, Henry Gutwirth Fund, MJRG, BMBF, and Minerva. J.M.L.M. is a member of the Lise Meitner-Minerva Center for Computational Quantum Chemistry and holds the Baroness Thatcher Professorial Chair in Chemistry. M.E.vdB. holds the Dewey David Stone and Harry Levine Career Development Chair and is a Yigal Allon fellow.

**Supporting Information Available:** Experimental and computational details, crystallographic data, Cartesian coordinates of calculated structures, and complete ref 19. This material is available free of charge via the Internet at <http://pubs.acs.org>.

## References

- Keane, J. M.; Harman, W. D. *Organometallics* **2005**, *24*, 1786.
- Harman, W. D. *Coord. Chem. Rev.* **2004**, *248*, 853.
- Cotton, F. A. *Acc. Chem. Res.* **1968**, *1*, 257.
- Iverson, C. N.; Lachicotte, R. J.; Müller, C.; Jones, W. D. *Organometallics* **2002**, *21*, 5320.
- Carbó, J. J.; Eistenstein, O.; Higgitt, C. L.; Klahn, A. H.; Maseras, F.; Oelckers, B.; Perutz, R. N. *J. Chem. Soc., Dalton Trans.* **2001**, 1452.
- Bach, I.; Pörschke, K.-R.; Goddard, R.; Kopiske, C.; Krüger, C.; Rufinska, A.; Seevogel, K. *Organometallics* **1996**, *15*, 4959.
- Sweet, J. R.; Graham, W. A. G. *Organometallics* **1983**, *2*, 135.
- Zingales, F.; Chiesa, A.; Basolo, F. *J. Am. Chem. Soc.* **1966**, *88*, 2707.
- Collman, J. P.; Hegedus, L. S.; Norton, J. R.; Finke, R. G. *Principles and Applications of Organotransition Metal Chemistry*; University Science Books: Mill Valley, CA, 1987.
- Stahl, S. S.; Labinger, J. A.; Bercaw, J. E. *J. Am. Chem. Soc.* **1996**, *118*, 5961.
- Northcutt, T. O.; Wick, D. D.; Vetter, A. J.; Jones, W. D. *J. Am. Chem. Soc.* **2001**, *123*, 7257.
- Amatore, C.; Fuxa, A.; Jutand, A. *Chem.–Eur. J.* **2000**, *6*, 1474.
- Cohen, R.; Weitz, E.; Martin, J. M. L.; Ratner, M. A. *Organometallics* **2004**, *23*, 2315.
- Senn, H. M.; Ziegler, T. *Organometallics* **2004**, *23*, 2980.
- Reinhold, M.; McGrady, J. E.; Perutz, R. N. *J. Am. Chem. Soc.* **2004**, *126*, 5268.
- Sundermann, A.; Uzan, O.; Martin, J. M. L. *Chem.–Eur. J.* **2001**, *7*, 1703.
- Goopen, L. J.; Koley, D.; Hermann, H.; Thiel, W. *Chem. Commun.* **2004**, 2141.
- Schunn, R. A. *Inorg. Chem.* **1976**, *15*, 208.
- Frisch, M. J. et al. *Gaussian 03*, revision C.01; Gaussian, Inc.: Pittsburgh, PA, 2004. Unless stated otherwise, all energies are at the PCM(THF)-BMK/SDB-cc-pVTZ//BMK/SDD level of theory.
- Boese, A. D.; Martin, J. M. L. *J. Chem. Phys.* **2004**, *121*, 3405.
- Harman, W. D.; Sekine, M.; Taube, H. *J. Am. Chem. Soc.* **1988**, *110*, 5725.
- Nunzi, F.; Sgamellotti, A.; Re, N. *J. Chem. Soc., Dalton Trans.* **2002**, 399.
- Bengali, A. A.; Leicht, A. *Organometallics* **2001**, *20*, 1345.

JA050613H